10780 *Biochemistry* **2010,** *49,* 10780–10787
DOI: 10.1021/bi101495x

BIOCHEMISTRY
including biophysical chemistry & molecular biology
Article

Characterization of Self-Association and Heteroassociation of Bacterial Cell Division Proteins FtsZ and ZipA in Solution by Composition Gradient−Static Light Scattering[†]

Ariadna Martos,[‡] Carlos Alfonso,[‡] Pilar López-Navajas,[‡] Rubén Ahijado-Guzmán,[‡] Jesús Mingorance,[§,⊥] Allen P. Minton,*[,∥] and Germán Rivas*[,‡]

[‡]*Chemical and Physical Biology Program, Centro de Investigaciones Biológicas, and* [§]*Department of Molecular Biotechnology, Centro Nacional de Biotecnología, Consejo Superior de Investigaciones Científicas, Madrid, Spain, and* [∥]*Section on Physical Biochemistry, Laboratory of Biochemistry and Genetics, National Institute of Diabetes and Digestive and Kidney Diseases, National Institutes of Health, Bethesda, Maryland 20892, United States.* [⊥]*Current address: Servicio de Microbiología, Hospital Universitario La Paz, IdiPAZ, Madrid, Spain.*

Received September 15, 2010; Revised Manuscript Received November 12, 2010

ABSTRACT: We have characterized the self-association of FtsZ in its GDP-bound state (GDP-FtsZ) and the heteroassociation of FtsZ and a soluble recombinant ZipA (sZipA) lacking the N-terminal transmembrane domain by means of composition gradient−static light scattering (CG−SLS) and by measurement of sedimentation equilibrium. CG−SLS experiments at high ionic strengths and in the presence of 5 mM Mg^{2+} show that, while FtsZ self-associates in a noncooperative fashion, sZipA acts as a monomer. CG−SLS data obtained from mixtures of FtsZ (A) and sZipA (B) in the presence of Mg^{2+} are quantitatively described by an equilibrium model that takes into account significant scattering contributions from B, A_1, A_2, A_3, A_4, A_5, A_6, A_1B, A_2B, A_3B, and A_4B. However, in the absence of Mg^{2+} (with EDTA), the data are best explained by an equilibrium model in which only B, A_1, A_2, A_3, A_1B, and A_2B contribute significantly to scattering. The best-fit molecular weights of monomeric A and B are in good agreement with values calculated from amino acid composition and with values obtained from sedimentation equilibrium. The latter technique also confirmed the interaction between sZipA and GDP-FtsZ. Moreover, the association model that best describes the CG−SLS data is in qualitative agreement with the sedimentation data. From these results, it follows that the binding of sZipA to GDP-FtsZ is of moderate affinity and does not significantly affect the interactions between FtsZ monomers. Under the working conditions used, only one sZipA binds to FtsZ oligomers with a length of six at most. The observed behavior would be compatible with FtsZ fibrils being anchored in vivo to the bacterial inner plasma membrane by substoichiometric binding of membrane-bound ZipA.

The components of the bacterial cell division machinery assemble in a concerted manner to form a dynamic ring at midcell toward the end of the cell cycle. The ring is formed by at least 15 division specific proteins, most of them integral membrane proteins. The first multiprotein complex formed is the bacterial proto-ring that initiates division. In *Escherichia coli*, the proto-ring is a complex of three proteins (FtsZ, FtsA, and ZipA) assembling on the cytoplasmic membrane that are required for the incorporation of the remaining proteins into the mature ring (*1*) (*2*). The best characterized proto-ring protein is FtsZ, which shares structural, but not sequence, homology with eukaryotic tubulin, as well as its GTPase activity and its capacity to polymerize (*3*) (*4*). In its GDP-bound state, the FtsZ monomer self-associates in a noncooperative manner to form oligomers, a reaction that is promoted by magnesium, low pH, and excluded volume effects in highly crowded media and that it is attenuated with an increase in solution ionic strength (*5*−*7*). GTP triggers FtsZ assembly in vitro to form polymers whose structural organization is highly polymorphic (single-stranded protofilaments, circles, toroidal structures, bundles, etc.) depending upon the solution composition and experimental conditions (*5*, *7*−*14*). The GTP-mediated assembly−disassembly cycle of FtsZ is thought to be essential for the formation of the dynamic septal ring during cell division (*2*−*4*, *15*).

FtsZ is anchored to the cytoplasmic membrane through the interaction of its carboxy-terminal region with ZipA or FtsA. FtsA belongs to the actin family and contains a short amphipathic helix that seems to mediate its association with the membrane (*16*). *E. coli* ZipA is a 36.4 kDa protein that contains an amino-terminal helix that is integrated into the membrane and connected to a cytoplasmic FtsZ-interacting domain via a flexible linker (*17*−*20*). FtsA and ZipA are involved in the attachment of FtsZ to the membrane, but no localization of FtsZ occurs in the simultaneous absence of both. In fact, under normal conditions, ZipA is required and essential for *E. coli* Z-ring formation (*21*). ZipA stabilizes GTP-FtsZ polymers in vitro and in vivo that might be related to

[†]This work was supported by Plan Nacional (Ministerio de Ciencia e Innovación, Spain) Grants BIO2008-04478-C03 to G.R. Grant DIVINOCELL FP/HEALTH-F3-2009-223432 (European Commision) to G.R., and Grant COMBACT S-BIO-0260/2006 (Comunidad de Madrid) to J.M. and G.R. A.M. is a predoctoral fellow from the Ministerio de Ciencia e Innovación of Spain. P.L.-N. was a recipient of a predoctoral fellowship from the Comunidad de Madrid. The research of A.P.M. is supported by the Intramural Research Program of the National Institute of Diabetes and Digestive and Kidney Diseases. J.M. was the recipient of a Ramón y Cajal fellowship financed by the Spanish Ministerio de Ciencia e Innovación and the European Social Fund.

*To whom correspondence should be addressed. G.R.: Centro de Investigaciones Biológicas, CSIC, Ramiro de Maeztu 9, E-28040 Madrid, Spain; e-mail, grivas@cib.csic.es; telephone, 34918373112; fax, +34 915360432. A.P.M.: National Institutes of Health, Building 8, Room 226, Bethesda, MD 20892; e-mail, minton@helix.nih.gov; telephone, (301) 496-3604.

 Published on Web 11/17/2010

the effect of ZipA on the bundling of FtsZ polymers, in which the C-terminal domain seems to be involved (*19*, *22*) . The interaction between FtsZ and ZipA has been studied by means of genetic and structural approaches (*17*−*27*), but the mechanism of association between the two proteins is largely unknown. The only quantitative information about formation of the ZipA−FtsZ complex was reported by Mosyak and co-workers (*26*). They used surface plasmon resonance to measure the binding of a 17-amino acid region from the C-terminal domain of FtsZ (in its GDP-bound state) to two soluble fragments of ZipA immobilized onto the sensor chip and found the interactions in the complexes were weak (apparent dissociation constants of $> 20\ \mu M$); these interactions did not change when the two protein fragments were in solution, as measured by isothermal titration calorimetry.

The aim of this work was the biophysical analysis of the association between ZipA and GDP-FtsZ in solution to measure the binding parameters of formation of the ZipA−FtsZ complex. This information is important for undertaking the quantitative characterization of these multiprotein complexes at different levels of organization (like reconstituted and natural membrane systems). We first isolate and analyze the full-length ZipA protein in the absence of detergent. We found that detergent-free ZipA existed mainly as a 16S oligomer, much larger than the expected *s* value of the monomer (∼3 S) and compatible with a 450−500 kDa globular oligomer (ZipA decamer). Upon incubation with GDP-FtsZ, the oligomers of ZipA formed large aggregates, observations also confirmed by electron and atomic force microscopy. These results hampered the use of full-length ZipA for a quantitative study of binding to FtsZ in solution. However, from these preliminary studies, we concluded that ZipA in solution retained the capacity of binding to FtsZ, with moderate affinity ($K > 10^5\ M^{-1}$). We also found, by means of electron microscopy and differential centrifugation assays, that full-length ZipA in a low-salt buffer (with 50 mM KCl, but not with 500 mM) promoted the formation of FtsZ polymer bundles at substoichiometric concentrations of ZipA, results that confirm previous studies conducted in lower-pH buffers with 0.05 M KCl (*19*) . To overcome these technical difficulties associated with the tendency of ZipA to aggregate, we have generated a soluble fragment of the protein that does not contain the transmembrane region (sZipA) and measured the binding of sZipA and GDP-FtsZ in solution by means of recently developed composition gradient−static light scattering methods in combination with sedimentation equilibrium measurements. The former technique is a new powerful tool for rapidly and accurately measuring protein self-association and heteroassociation in solution (*28*−*32*). In composition gradient−static light scattering (CG−SLS) experiments, light scattering data are acquired from a solution whose composition is being continuously varied with time in a controlled fashion. The resulting profiles of light scattering intensity as a function of solution composition are then modeled in the context of schemes postulating different combinations of self-association and/or heteroassociation equilibria, to determine the simplest scheme capable of accounting for the data to within experimental precision. This approach has allowed us to define the scheme of association between sZipA and FtsZ as well as the affinity and stoichiometry of the different species present in the solution. Finally, the potential implications of these results for understanding the association of FtsZ with ZipA at the cytoplasmic membrane are discussed.

EXPERIMENTAL PROCEDURES

Materials. All the assays described in this paper were conducted at 25 °C with the proteins equilibrated in 50 mM Tris-HCl (pH 7.4) and 500 mM KCl buffer, with either 5 mM $MgCl_2$ (Tris-500KCl-Mg buffer) or 1 mM EDTA (Tris-500KCl-EDTA buffer), in the presence of the nucleotide (GDP or GTP) specified in the text. Guanine nucleotides, GDP and GTP, were purchased from Sigma-Aldrich and Roche, respectively. Other analytical grade chemicals were from Merck or Sigma.

Proteins. *E. coli* FtsZ was purified by the Ca^{2+}-induced precipitation method described by Rivas et al. (*7*). In this study, we have mainly used FtsZ in the GDP-bound state (nonpolymerized protein), and we will call it GDP-FtsZ.

Mutagenesis of the zipA Gene and Overexpression and Purification of sZipA. A soluble mutant of ZipA was constructed by elimination of the hydrophobic N-terminal domain (amino acids 1−25) of the full-length protein. The deletion was obtained by inverse polymerase chain reaction (PCR) using plasmid pET-15ZIP as template DNA and primers 5′-CATATGGCT-GCCGCGCG-3′ and 5′-ACCAGCCGTAAAGAACG-3′. The PCR product was purified, digested with *Dpn*I, and ligated with T4 DNA ligase. The presence of the desired deletion and the absence of other mutations were checked by DNA sequencing.

To overproduce sZipA, BL21/DE3 cells transformed with pET-15ZIP (*22*) were grown at 37 °C in LB supplemented with ampicillin (50 μg/mL) and chloramphenicol (50 μg/mL), yielding an optical density of 0.4. Protein expression was induced with 1 mM IPTG for 3 h. Cells were harvested, centrifuged at 10000*g* (4 °C for 15 min), and resuspended in 0.02 culture volume of buffer A [20 mM Tris-HCl (pH 8.0), 500 mM NaCl, and 5 mM imidazole]. After sonication, cell extracts were centrifuged at 200000*g* (4 °C for 30 min) to pellet membranes. sZipA was recovered from the soluble fraction and loaded on a 5 mL Ni-NTA resin (Novagen) equilibrated in buffer A. The protein was eluted sequentially with 50, 100, 200, and 500 mM imidazole in buffer A. Most of the sZipA protein eluted with 200 mM imidazole. The protein concentration was determined by the Bradford assay. The protein yield was typically 4−6 mg of sZipA/L of cell culture. sZipA fractions were pooled and stored at −80 °C. The purity of sZipA was >90% according to sodium dodecyl sulfate−polyacrylamide gel electrophoresis.

Static Light Scattering. Composition gradient−static light scattering experiments were performed using the Calypso system (Wyatt Technology, Santa Barbara, CA) according to procedures developed by Minton and co-workers (*30*−*32*). In brief, a programmable three-injector syringe pump was used to introduce a solution with a defined protein composition (that changes with time) into parallel flow cells for concurrent measurement of Rayleigh light scattering at multiple angles (using a DAWN-EOS multiangle laser light scattering detector from Wyatt Technology) and solute composition (using a Optilab rEX refractive index detector from Wyatt Technology). A single-composition gradient experiment yields several thousand values of scattering intensity as a function of scattering angle and solution composition. The specific refractive increments of FtsZ and sZipA were measured using an Optilab rEX differential refractometer (Wyatt Technology), and both were found to be equal to $0.185 \pm 0.002\ cm^3/g$ at 25 °C.

Experiments with a single protein were performed as described by Attri and Minton (*31*). One of the pump channels (syringe and reservoir) was filled with a solution of either GDP-FtsZ or sZipA and a second with a buffer solution. Stepwise gradients of increasing

or decreasing protein concentration were formed by increasing in incremental intervals the flow rate of one of the syringes and simultaneously decreasing by the same amount the flow rate of the other syringe. Experiments with mixtures of two proteins were performed as described by Attri and Minton (*30*). A solution of sZipA (solution B) at weight-to-volume concentration $w_{B,load}$ was loaded into one of the pump channels, and a solution of GDP-FtsZ (solution A) at weight-to-volume concentration $w_{A,load}$ was loaded into the second pump channel. Initially, the flow cells were filled with pure solution B, permitting determination of the scattering intensity at multiple angles and absorbance of sZipA at the loading concentration. Composition gradients were created by simultaneously increasing the flow rate of pump channel A and decreasing the flow rate of pump channel B; as a result, the fraction of solution B in the solution mixture gradually decreases from 1 to 0 while that of solution A gradually increases from 0 to 1. Absorbance data were processed to yield the concentration of either one protein (in a single-protein experiment) or both proteins (in a two-protein experiment), as described in refs *30* and *31*. The scattering data were processed as previously described by Attri and Minton (*30*, *31*) to yield the Rayleigh ratio R scaled to an optical constant

$$K_{opt} = \frac{4\pi\tilde{n}^2(\mathrm{d}\tilde{n}/\mathrm{d}w)^2}{\lambda^4 N_A} \quad (1)$$

where λ, N_A, and $\tilde{n}$ denote the wavelength of incident light (690 nm), Avogadro's number, and the refractive index of the solution, respectively. $\mathrm{d}\tilde{n}/\mathrm{d}w$ is the specific refractive increment of both proteins, determined as described above, where w denotes the weight-to-volume concentration of the protein. In this study, all solute species were small relative to the wavelength of light. Therefore, the scaled Rayleigh ratio is independent of scattering angle and depends only upon the solute composition:

$$\frac{R}{K_{opt}} = \sum_i M_i w_i = \sum_i c_i M_i^2 \quad (2)$$

where M_i, w_i, and c_i denote the molar mass, the weight-to-volume concentration, and the molar concentration of the ith solute species, respectively. The fractional contribution of a given species to the total scattering intensity is then given by

$$f_j = \frac{c_j M_j^2}{\sum_i c_i M_i^2} \quad (3)$$

The composition dependence of R/K_{opt} is modeled in the context of equilibrium schemes described below that specify the molar masses of all significant scattering species, and the dependence of all c_i values upon one or more postulated equilibrium association constants and the total concentrations of each protein or both proteins.

Models for Equilibrium Self-Association and Heteroassociation. Several equilibrium models were constructed to calculate the molar concentration of each macromolecular species present as a function of the total concentration of each macromolecular component and one or more equilibrium association constants. The results of these models were then combined with eq 2 to calculate the dependence of total scattering upon solution composition. Below we describe the simplest models found to describe the data obtained in this study within experimental uncertainty. In a solution containing only a single protein component (A), the subscript i denotes a property of the oligomeric species A_i. In a solution containing two protein components (A and B), the subscript ij denotes a property of the oligomeric species A_iB_j.

Model 1: Isodesmic Model for Self-Association of GDP-FtsZ (*component A*). It is assumed that monomeric A may bind to another monomer or any oligomer of A with equal affinity.

$$K_{AA} = c_{i+1}/c_1 c_i \quad \text{for all } i \quad (4)$$

$$c_{tot} = \frac{w_{tot}}{M_1} = \sum_{i=1}^{\infty} i c_i = \frac{1}{K_{AA}} \sum_{i=1}^{\infty} i(K_{AA}c_1)^i = \frac{1}{K_{AA}} \frac{q}{(1-q)^2} \quad (5)$$

where $q \equiv K_{AA}c_1$. Given values of w_{tot}, M_1, and K_{AA}, one may solve eq 5 for the values of q and c_1. It follows from eq 2 that the normalized scattering is then given by

$$\frac{R}{K_{opt}} = \sum_{i=1}^{\infty} c_i(iM_1)^2 = \frac{M_1^2}{K_{AA}} \sum_{i=1}^{\infty} i^2(K_{AA}c_1)^i = \frac{M_1^2}{K_{AA}} \times \frac{q+q^2}{(1-q)^3} \quad (6)$$

Model 2: Isodesmic Self-Association of GDP-FtsZ (*component A*) *and Heteroassociation of Each Oligomeric Species of A with One or Two Molecules of sZipA* (*component B*). It is assumed that one or two molecules of B may bind to a monomer or any oligomer of A with an affinity that is independent of the size of the oligomer. The second molecule of B binds to monomeric or oligomeric A with an equilibrium constant for association that differs from the equilibrium constant for binding the first B by a factor α.

$$K_{AA} = \frac{c_{(i+1)0}}{c_{i0}c_{10}} \quad \text{for all } i \quad (7)$$

$$K_{AB} = \frac{c_{i1}}{c_{i0}c_{01}} \quad \text{for all } i \quad (8)$$

$$\alpha K_{AB} = \frac{c_{i2}}{c_{i1}c_{01}} \quad \text{for all } i \quad (9)$$

The conservation of mass equations may be written as

$$c_{A,tot} = \frac{w_{A,tot}}{M_{10}} = (1 + B^* + \alpha B^{*2}) \frac{1}{K_{AA}} \frac{A^*}{(1-A^*)^2} \quad (10)$$

$$c_{B,tot} = \frac{w_{B,tot}}{M_{01}} = c_{01} + (B^* + 2\alpha B^{*2}) \frac{1}{K_{AA}} \frac{A^*}{1-A^*} \quad (11)$$

where $A^* = K_{AA}c_{10}$ and $B^* = K_{AB}c_{01}$. Given values of $w_{A,tot}$, $w_{B,tot}$, M_{10}, M_{01}, K_{AA}, K_{AB}, and α, one may solve eqs 10 and 11 numerically for the equilibrium values of c_{10} and c_{01}. Then eqs 7−9 may be used to calculate the all equilibrium values of c_{ij}. The corresponding value of R/K_{opt} is calculated numerically by summing over all significantly populated species in the following special case of eq 2

$$\frac{R}{K_{opt}} = c_{01}M_{01}^2 + \sum_{i=1}^{\infty} \sum_{j=0}^{2} c_{ij}(iM_{10} + jM_{01})^2 \quad (12)$$

When the infinite sum indicated above was evaluated, terms in increasing i were successively added until convergence was established.

All data processing and modeling calculations were performed using user-written scripts and functions written in MATLAB (Mathworks, Natick, MA) available from A.P.M. upon request.

Sedimentation Equilibrium. Sedimentation equilibrium was assessed to determine the state of association of the individual components (sZipA and GDP-FtsZ) and to measure the association properties of sZipA−FtsZ complexes. The analytical

ultracentrifugation analysis of sZipA, GDP-FtsZ, and the sZipA−FtsZ mixtures was performed using several protein concentrations (in the range of 0.3−1 g/L) equilibrated in either Tris-500KCl-Mg or Tris-500KCl-EDTA buffer containing 0.05 mM GDP. Sedimentation velocity runs were conducted at 42000 rpm and 25 °C. Sedimentation profiles were registered every 5 min at the appropriate wavelength (230 or 275 nm). Short-column (70−80 μL) experiments were conducted at 25 °C in an XL-A analytical ultracentrifuge (Beckman-Coulter Inc.) with a UV−vis optics detection system, using an An60Ti rotor and 12 mm double-sector centerpieces. The equilibrium runs were conducted at two speeds (10000 and 12000 rpm), and the gradients were monitored at two different wavelengths (230 and 275 nm). Following the equilibrium scans, the solutions were centrifuged at high speed (40000 rpm) to deplete the meniscus and obtain the corresponding baseline offsets. The measured equilibrium concentration (signal) gradients of sZipA and FtsZ alone were fit by the equation that characterizes the equilibrium gradient of an ideally sedimenting solute (*33*), yielding the whole-cell buoyant signal average molecular weights of the individual proteins.

Analysis of Sedimentation Equilibrium Data. For two components (A being FtsZ and B being sZipA), the absorbance average molecular weight is given by (*34*)

$$M_{\mathrm{abs,av}} = \frac{\sum_{i,j}(iM_{\mathrm{A}}\alpha_{\mathrm{A}} + jM_{\mathrm{B}}\alpha_{\mathrm{B}})c_{ij}(iM_{\mathrm{A}} + jM_{\mathrm{B}})}{\sum_{i,j}(iM_{\mathrm{A}}\alpha_{\mathrm{A}} + jM_{\mathrm{B}}\alpha_{\mathrm{B}})c_{ij}} \quad (13)$$

where M_{X} is the molecular weight of monomeric X, α_{X} is the extinction coefficient of X at the wavelength of measurement, and c_{ij} is the molar concentration of $\mathrm{A}_i\mathrm{B}_j$. If the two components have the same density increment ($\mathrm{d}\rho/\mathrm{d}w_{\mathrm{A}} = \mathrm{d}\rho/\mathrm{d}w_{\mathrm{B}} = \mathrm{d}\rho/\mathrm{d}w$), then the experimentally measured buoyant signal average molecular weight is just $M^*_{\mathrm{abs,av}} = M_{\mathrm{abs,av}}(\mathrm{d}\rho/\mathrm{d}w)$. A MATLAB function using eqs 7−11 and 13 was written to calculate the buoyant absorbance average molecular weight as a function of the total weight-to-volume concentrations of A and B.

It follows from eqs 2, 6, and 12 that any equilibrium model used to generate a calculated dependence of R/K_{opt} upon protein concentration may also be used to generate a calculated dependence of M_{w} upon protein concentration, which is the form of the sedimentation equilibrium results presented in this work. Therefore, with minor modifications, the same association schemes described above to model the composition dependence data of light scattering can also be used to model the composition dependence data of sedimentation equilibrium experiments.

RESULTS AND DISCUSSION

sZipA. The normalized scattering intensity of sZipA in the absence and presence of Mg^{2+} is plotted as a function of protein concentration in Figure 1. Both sets of data are fit quantitatively by a model according to which sZipA behaves as a single species with an M_{w} of 34000 ± 1000, in good agreement with the sequence molecular weight of the monomer (35829). The best fit of this model to each data set is plotted together with the data. It follows that sZipA does not self-associate to a significant extent in either buffer over the measured range of concentrations. We confirmed that sZipA was a monomer in solution by analytical ultracentrifugation (Figure 2). The buoyant average molecular weight of sZipA, determined by sedimentation equilibrium, was 9500 ± 1000 (M_{w} = 36000, calculated using 0.736 cm^3/g as the partial specific volume of sZipA), corresponding to a protein monomer. The sedimentation properties of sZipA did not change when the KCl concentration was decreased to 0.05 M or when EDTA was added to the buffer (not shown).

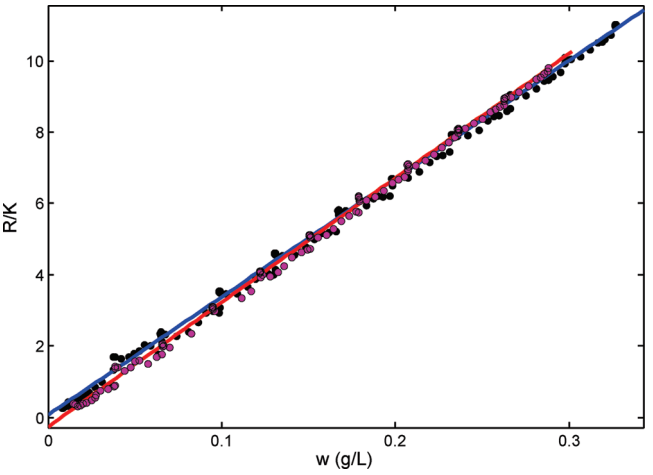

FIGURE 1: Normalized scattering intensity plotted as a function of sZipA concentration in the absence (black symbols) and presence (red symbols) of 5 mM Mg^{2+}. The blue line is the best fit of a single-species model with an M_{w} of 34000 ± 1000.

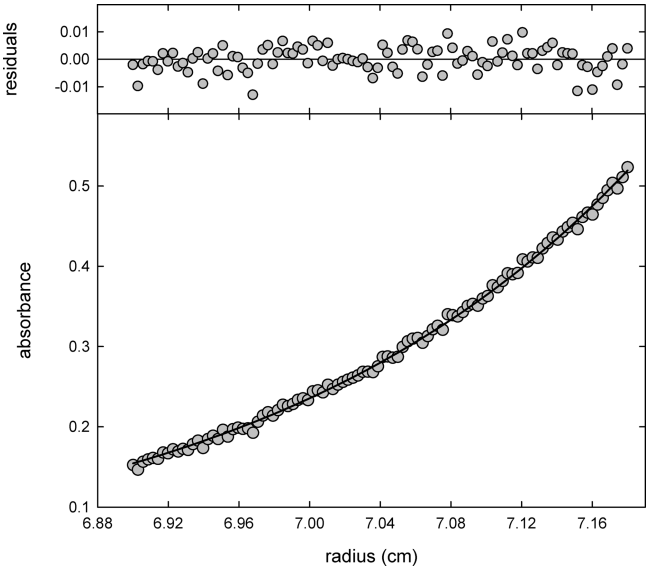

FIGURE 2: Analytical ultracentrifugation analysis of sZipA. Sedimentation equilibrium absorbance gradient of 14 μM sZipA at 12000 rpm. The solid line is the best-fit distribution from the single-species model with an M_{w} of 36000 ± 2000, which corresponds to a protein monomer.

GDP-FtsZ. The concentration-dependent scattering of FtsZ in (high salt) Tris-500KCl buffer in the absence and presence of Mg^{2+} is plotted in Figure 3. Both sets of data are fit quantitatively by the isodesmic self-association model described above. The best fit of this model to each data set, calculated using the parameter values given in the figure caption, is plotted together with the data. The fractional contribution of each significant species to the total scattering, calculated according to eq 3, is plotted as a function of total protein concentration, and the corresponding mass fractional distributions are plotted in Figures S1 and S2 of the Supporting Information, respectively. In the presence of Mg^{2+}, the scattering data are well described for by an equilibrium model that takes into account significant scattering contributions

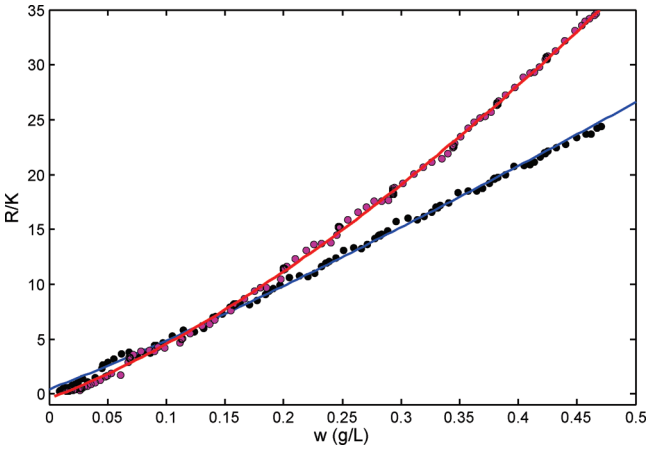

FIGURE 3: Normalized scattering intensity plotted as a function of GDP-FtsZ concentration in the absence (black symbols) and presence (red symbols) of 5 mM Mg^{2+}. Plotted curves represent the best fits of model 1 with an M_1 of 40000 (constrained) and log K_{AA} values of 4.3 (without Mg^{2+}) and 4.8 (with Mg^{2+}).

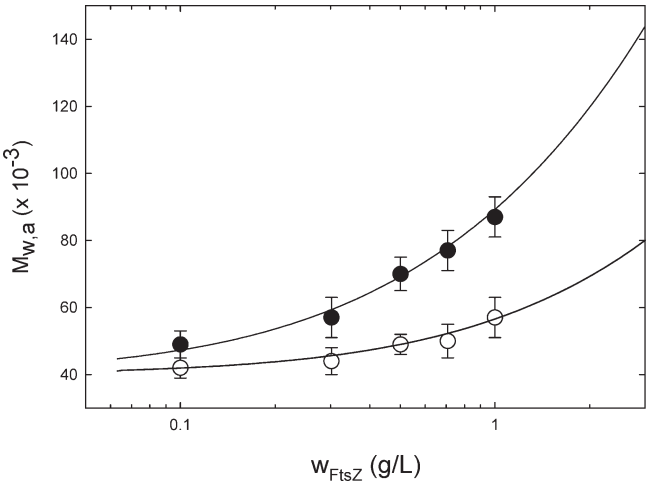

FIGURE 4: Dependence of the signal-average molecular weight of GDP-FtsZ on protein concentration in the absence (○) and presence (●) of 5 mM Mg^{2+} measured by sedimentation equilibrium. The plotted curves represent the best fits of model 1 with an M_1 of 40000 (constrained) and log K_{AA} values of 4.2 (without Mg^{2+}) and 4.7 (with Mg^{2+}).

of several FtsZ species, from monomers to hexamers. In the presence of EDTA, FtsZ self-association is attenuated, as expected, and only monomers, dimers, and trimers contributed to the scattering signal.

In parallel, we conducted low-speed sedimentation equilibrium analysis with the same FtsZ preparations (loading concentrations ranging from 0.3 to 1.0 g/L, or from 7.5 to 25 μM) that yielded signal buoyant average molecular weights from 15200 to 21800 (M_w from 57000 to 82000, calculated using 0.738 cm^3/g as the partial specific volume of FtsZ) (for the protein in 5 mM Mg^{2+}) and from 11200 to 14600 (M_w from 42000 to 55000) (EDTA). The dependence of the molecular weight of FtsZ on total protein concentration confirmed the results obtained in previous studies from our laboratory (*5*) and, more importantly, is in good quantitative agreement with the isodesmic model that accounts for the results obtained from composition gradient−light scattering (CG−LS) (Figure 4).

sZipA and GDP-FtsZ. We then conducted composition gradient−light scattering to detect and quantify the association between GDP-FtsZ and sZipA. A 0.35 g/L solution of ZipA (B) was automatically mixed in various proportions with a 0.5 g/L solution of FtsZ (A), to produce a gradient with a composition continuously varying from mole fraction 0 to mole fraction 1 of A. The normalized scattering of these mixtures, in the absence and presence of Mg^{2+}, is plotted as a function of the fraction of solution A in the mixture in Figure 5.

Both sets of data are fit quantitatively by model 2 and exclude the binding of more than one molecule of B (sZipA) to each monomer or oligomer of A (FtsZ). In this model, it is assumed that GDP-FtsZ self-associates isodesmically (with equal stepwise equilibrium constants for addition of monomer to oligomer). This is the model that satisfactorily describes the self-association of GDP-FtsZ in the absence of sZipA (see below and ref *32*). In addition, it allows for the possibility of binding either one or two molecules of sZipA to each monomer or oligomer of GDP-FtsZ. The binding constant for the binding of the first molecule of sZipA is K_{AB}, and the binding constant for binding of the second molecule is αK_{AB}. The data indicate that the binding of one molecule of sZipA to an oligomer of FtsZ reduces the affinity for binding of a second molecule of sZipA to the same oligomer by a factor of > 10 ($\alpha < 0.03$). The best fit of this model to each data

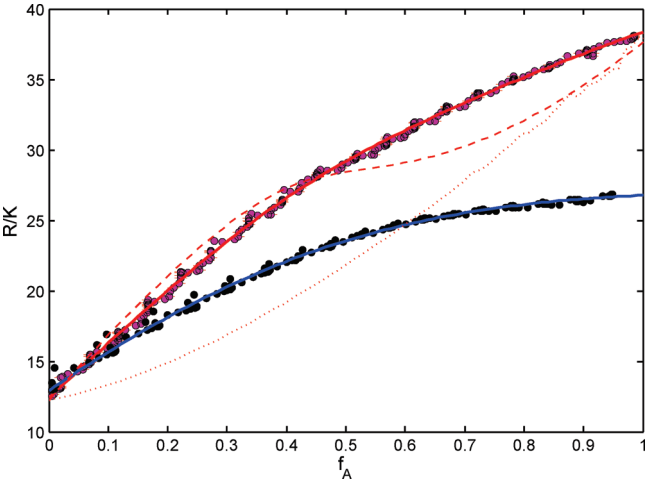

FIGURE 5: Normalized scattering intensity plotted as a function of the fraction of solution A (0.5 g/L FtsZ) mixed with solution B (0.35 g/L sZipA) in the absence (black symbols) and presence (red symbols) of 5 mM Mg^{2+}. Plotted solid lines represent the best fits of model 2 with the following values: $M_A = 40000$, $M_B = 35000$, log $K_{AA} = 4.18 \pm 0.02$ (EDTA) or 4.79 ± 0.02 (with Mg^{2+}), log $K_{AB} = 5.24 \pm 0.07$ (EDTA) or 5.78 ± 0.20 (with Mg^{2+}), and $\alpha < 0.1$ (EDTA) or $\alpha < 0.03$ (with Mg^{2+}). The dashed and dotted lines represent the calculated dependence of scattering (with Mg^{2+}) upon fA, assuming binding of B only to monomeric A (no binding to oligomeric A) and no binding of B to A in any form, respectively.

set, calculated using the parameter values given in the figure caption (see also Table 1), is plotted in Figure 5 together with the data. The best-fit values of K_{AA} obtained from the analysis of the mixtures of FtsZ and sZipA are in very good agreement with those previously obtained from the concentration dependence of the light scattering of GDP-FtsZ in the absence of sZipA under comparable conditions. This lends confidence to the robustness of our more general analysis of the two-component systems. The best-fit values of log K_{AA} and log K_{AB} are well-defined by the data, assuming that the concentrations and molecular weights of the two proteins have the assumed values. Even if the concentrations and molecular weights were slightly uncertain, the best-fit values of log K_{AA} and log K_{AB} were still well-defined, however, with tolerances somewhat larger than those presented in the legend

Table 1: Equilibrium Association Values for Self-Association and Heteroassociation of FtsZ and sZipA As Determined by Composition Gradient−Static Light Scattering (CG−SLS) and Sedimentation Equilibrium (SE)[a]

protein	Mg^{2+}	log K_{AA}	log K_{AB}	α
FtsZ (A)	no	4.2 ± 0.1 (LS1)		
FtsZ (A) and sZipA (B)	no	4.18 ± 0.02 (LS2), 3.8 (SE2)	5.24 ± 0.02 (LS2), 5.1 (SE2)	< 0.1 (LS2), 0 (SE2)
FtsZ (A)	yes	4.7 ± 0.1 (LS1)		
FtsZ (A) and sZipA (B)	yes	4.79 ± 0.02 (LS2), 4.6 (SE2)	5.78 ± 0.02 (LS2), 5.4 (SE2)	< 0.03 (LS2), 0 (SE2)

[a]Legend: no, experiment conducted in the presence of 1 mM EDTA; +, experiment conducted in the presence of 5 mM $MgCl_2$; LS1, best-fit parameter values from the analysis of the CG−LS data using model 1 (eqs 4−6), with an M_A of 40000; SE1, best-fit parameter values from the analysis of the sedimentation equilibrium data using model 1 (eqs 4, 5, and 13), with an M_A of 40000; LS2, best-fit parameter values from the analysis of the CG−LS data using model 2 (eqs 7−12), with an M_A of 40000 and an M_B of 35000; SE2, best-fit parameter values from the analysis of the sedimentation equilibrium data using model 2 (eqs 7−11 and 13), with an M_A of 40000 and an M_B of 35000.

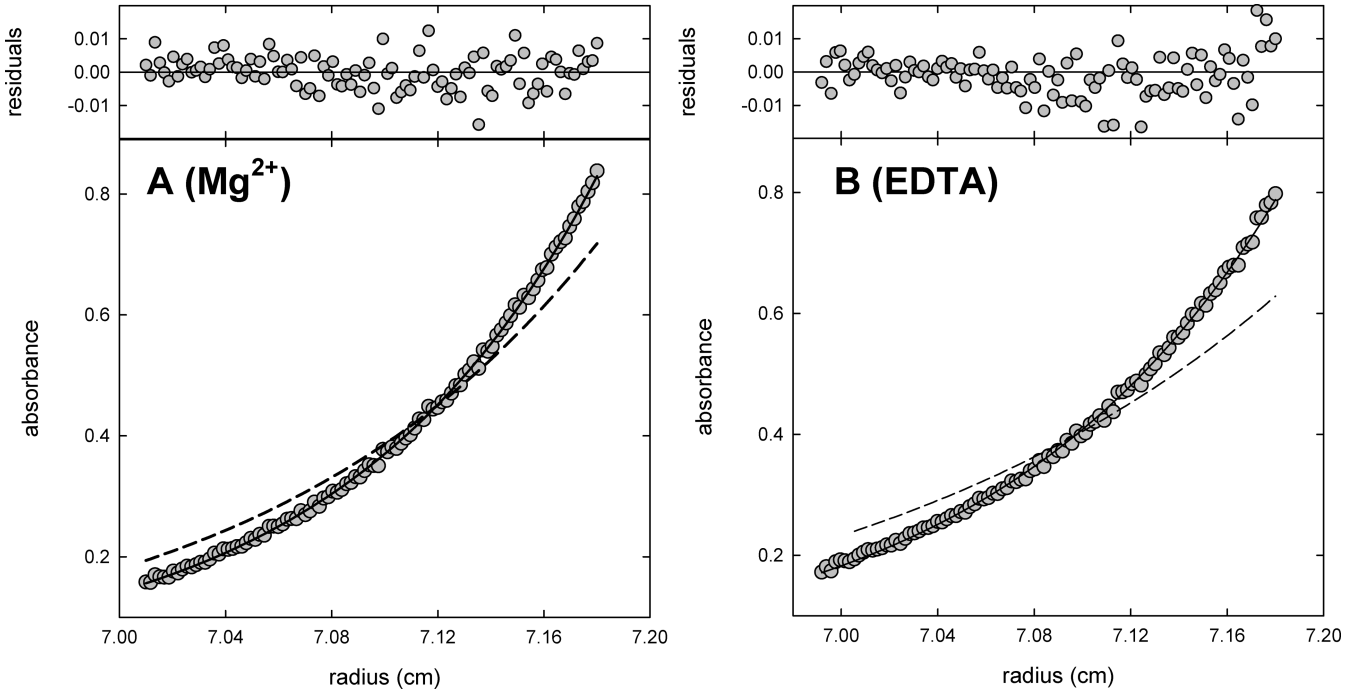

FIGURE 6: Sedimentation equilibrium analysis of binding of sZipA to GDP-FtsZ. Sedimentation equilibrium absorbance profiles obtained at a rotor speed of 10000 rpm and 20 °C for a sZipA−FtsZ mixture (each protein at 0.5 g/L) equilibrated in Tris-500KCl buffer containing either 5 mM $MgCl_2$ (A) or 1 mM EDTA (B). Solid lines are the best-fit equilibrium gradients for an ideally sedimenting species with signal average buoyant M_w values of 19000 ± 800 (Mg^{2+}) and 15700 ± 1000 (EDTA). The dashed lines are the predicted gradients of the noninteracting mixture at the same protein concentration in the presence and absence of Mg^{2+}, respectively.

of Figure 5. To illustrate how sensitive the results are to variation in model parameters, the CG−LS profiles of the mixture assuming either no binding of sZipA to FtsZ (dotted line) or binding of sZipA only to monomeric FtsZ (dashed line) are also plotted in Figure 5.

The fractional contribution of each species to total scattering in the absence of Mg^{2+}, calculated according to eq 3, and the corresponding mass fractional distributions are plotted as a function of solution composition in Figures S3 and S4 of the Supporting Information, respectively. The fractional distribution plots in the presence of 5 mM Mg^{2+} are shown in Figures S5 and S6 of the Supporting Information. From these results, we concluded that the scattering data obtained in the presence of Mg^{2+} are fit by an equilibrium model that takes into account significant scattering contributions not only of the species that can be observed in the EDTA (B, A, A_2 A_3, AB, and A_2B) but also of A_4, A_5, A_6, A_3B, and A_4B.

We confirmed the interaction between sZipA and GDP-FtsZ by low-speed sedimentation equilibrium. Figure 6 shows the equilibrium gradients of the mixture of sZipA (0.5 g/L, 14 μM) and FtsZ (0.5 g/L, 12.5 μM) obtained in Tris-500KCl buffer with either 5 mM Mg^{2+} (panel A) or 1 mM EDTA (panel B) together with the calculated best-fit gradients assuming a single-species model. The data are described well by species with single average buoyant M_w values of 19000 ± 800 (Mg^{2+}) and 15700 ± 1000 (EDTA), values that in both cases are significantly higher than the signal average buoyant M_w of the noninteracting mixtures (14200 ± 1000 with Mg^{2+} and 10500 ± 1000 with EDTA), calculated from the buoyant M_w measured in parallel for isolated sZipA and FtsZ at the same concentration, in the presence and absence of Mg^{2+}. These results demonstrated the presence of heterocomplexes under the two experimental conditions studied. The analysis of the dependence of the average molecular weight as a function of the sZipA and FtsZ concentrations in the mixtures, calculated using model 2 as described in Materials and Methods, is in qualitative agreement with the results obtained from composition gradient−light scattering (Figure 7). The model fits the data reasonably well, and both K_{AA} and K_{AB} appear to increase in the presence of Mg^{2+} (Table 1). However, the values of log K_{AA} and log K_{AB}, with one exception

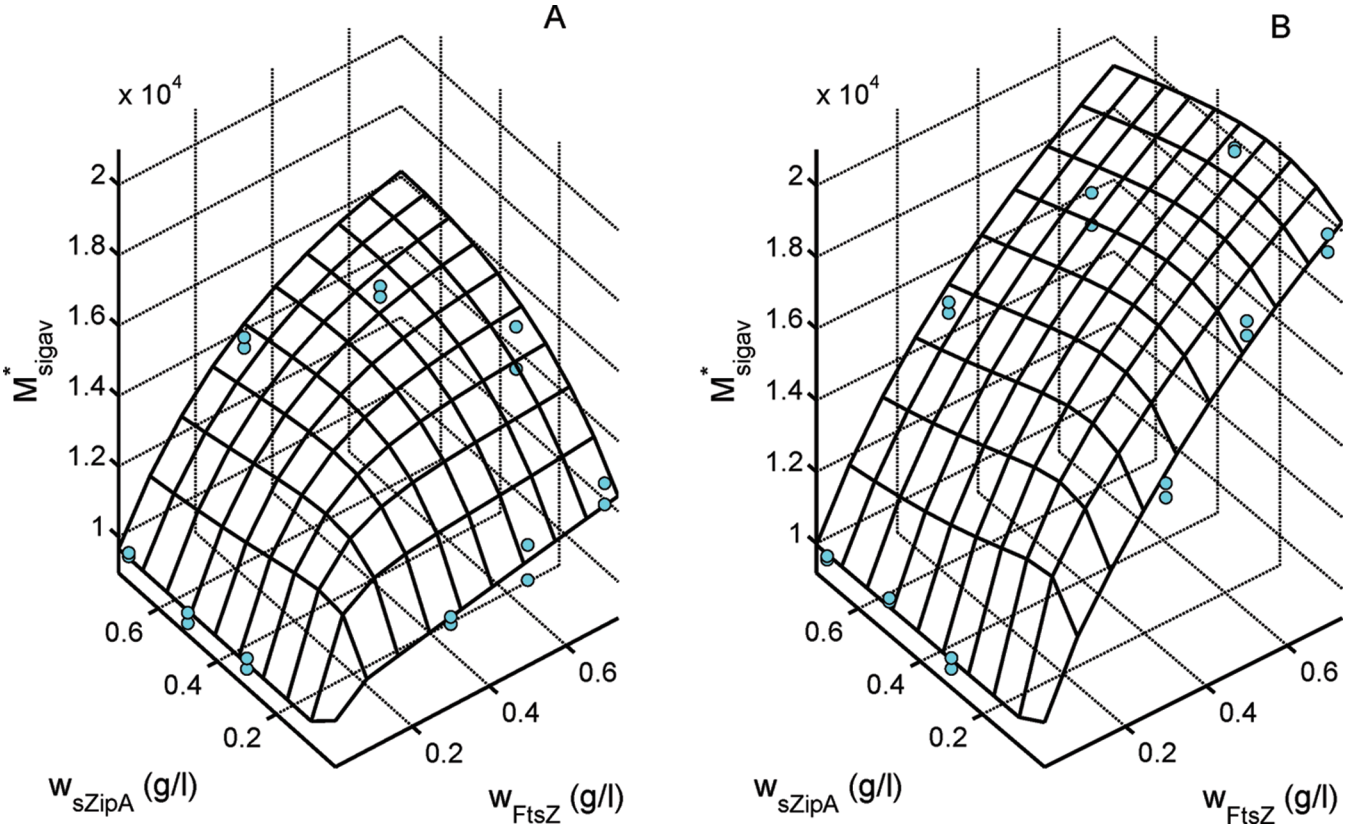

FIGURE 7: Analysis of the dependence of the signal average molecular weight of sZipA−FtsZ mixtures on sZipA (B) and FtsZ (A) concentrations as measured by sedimentation equilibrium: (A) 5 mM Mg^{2+} and (B) 1 mM EDTA. The grid lines represent the best fits of model 2 with the following values: $M_A = 40000$, $M_B = 35000$, log $K_{AA} = 3.8$ (without Mg^{2+}) or 4.6 (with Mg^{2+}), and log $K_{AB} = 5.1$ (without Mg^{2+}) or 5.4 (with Mg^{2+}).

(log K_{AB} in EDTA), are lower than the values obtained from the analysis of light scattering data.

CONCLUDING REMARKS

Our composition gradient−static light scattering study of ZipA−FtsZ mixtures of known composition has allowed us to determine that sZipA is monomeric and that one molecule sZipA can bind to a GDP-FtsZ monomer or oligomer (up to hexamers under our buffer conditions) with moderate affinity (Figure 7). These results are compatible with results of parallel measurements of composition-dependent sedimentation equilibrium. Moreover, they are in good agreement with earlier studies indicating that the C-terminal FtsZ-binding domain of ZipA binds with micromolar affinity to a C-terminal fragment of FtsZ (*26*). The observed dependence of the values of K_{AA} and K_{AB} upon Mg^{2+} concentration is probably more biologically relevant than the absolute values of these constants. Over the range of concentrations explored in our experiments, the largest FtsZ oligomer present at significant abundance is the hexameric species. Our data do not permit us to determine whether additional sZipA molecules can bind to larger GDP-FtsZ oligomers, but they establish that formation of the ZipA−FtsZ complex does not alter the self-association equilibrium between FtsZ molecules.

This work provides an additional example of the ability of the recently developed CG−SLS method to quantitatively characterize complex systems of self-association and/or heteroassociation equilibria in solutions containing one or two macromolecular components. Our conclusions are reinforced by parallel results obtained via measurements of sedimentation equilibrium. These results suggest a possible mechanism for anchoring of FtsZ fibers to the *E. coli* inner membrane via binding to membrane-localized ZipA.

ACKNOWLEDGMENT

We thank Prof. Miguel Vicente's group (CNB-CSIC) for technical support in preparing sZipA and for discussions.

SUPPORTING INFORMATION AVAILABLE

Fractional distributions of individual species to the total scattering intensity and weight fractional distribution of individual species plotted as a function of total concentration of GDP-FtsZ, in the absence and in the presence of Mg^{2+} (Figures S1 and S2, respectively) and fractional distributions of individual species to the total scattering intensity and weight fractional distributions of individual species in GDP-FtsZ−sZipA mixtures as a function of solution composition, in the absence and presence of Mg^{2+} (Figures S3−S6). This material is available free of charge via the Internet at http://pubs.acs.org.

REFERENCES

1. Vicente, M., and Rico, A. I. (2006) The order of the ring: Assembly of *Escherichia coli* cell division components. *Mol. Microbiol. 61*, 5–8.
2. Adams, D. W., and Errington, J. (2009) Bacterial cell division: Assembly, maintenance and disassembly of the Z ring. *Nat. Rev. Microbiol. 7*, 642–653.
3. Mingorance, J., Rivas, G., Velez, M., Gomez-Puertas, P., and Vicente, M. (2010) Strong FtsZ is with the force: Mechanisms to constrict bacteria. *Trends Microbiol. 18*, 348–356.
4. Dajkovic, A., and Lutkenhaus, J. (2006) Z ring as executor of bacterial cell division. *J. Mol. Microbiol. Biotechnol. 11*, 140–151.
5. Gonzalez, J. M., Jimenez, M., Velez, M., Mingorance, J., Andreu, J. M., Vicente, M., and Rivas, G. (2003) Essential cell division protein FtsZ assembles into one monomer-thick ribbons under conditions resembling the crowded intracellular environment. *J. Biol. Chem. 278*, 37664–37671.
6. Rivas, G., Fernandez, J. A., and Minton, A. P. (2001) Direct observation of the enhancement of noncooperative protein self-assembly by macromolecular crowding: Indefinite linear self-association of

bacterial cell division protein FtsZ. *Proc. Natl. Acad. Sci. U.S.A. 98*, 3150–3155.
7. Rivas, G., Lopez, A., Mingorance, J., Ferrandiz, M. J., Zorrilla, S., Minton, A. P., Vicente, M., and Andreu, J. M. (2000) Magnesium-induced linear self-association of the FtsZ bacterial cell division protein monomer. The primary steps for FtsZ assembly. *J. Biol. Chem. 275*, 11740–11749.
8. Gonzalez, J. M., Velez, M., Jimenez, M., Alfonso, C., Schuck, P., Mingorance, J., Vicente, M., Minton, A. P., and Rivas, G. (2005) Cooperative behavior of *Escherichia coli* cell-division protein FtsZ assembly involves the preferential cyclization of long single-stranded fibrils. *Proc. Natl. Acad. Sci. U.S.A. 102*, 1895–1900.
9. Huecas, S., and Andreu, J. M. (2003) Energetics of the cooperative assembly of cell division protein FtsZ and the nucleotide hydrolysis switch. *J. Biol. Chem. 278*, 46146–46154.
10. Huecas, S., Llorca, O., Boskovic, J., Martin-Benito, J., Valpuesta, J. M., and Andreu, J. M. (2008) Energetics and geometry of FtsZ polymers: Nucleated self-assembly of single protofilaments. *Biophys. J. 94*, 1796–1806.
11. Chen, Y., Bjornson, K., Redick, S. D., and Erickson, H. P. (2005) A rapid fluorescence assay for FtsZ assembly indicates cooperative assembly with a dimer nucleus. *Biophys. J. 88*, 505–514.
12. Chen, Y., and Erickson, H. P. (2008) In vitro assembly studies of FtsZ/tubulin-like proteins (TubZ) from *Bacillus* plasmids: Evidence for a capping mechanism. *J. Biol. Chem. 283*, 8102–8109.
13. Erickson, H. P., and Stoffler, D. (1996) Protofilaments and rings, two conformations of the tubulin family conserved from bacterial FtsZ to α/β and γ tubulin. *J. Cell Biol. 135*, 5–8.
14. Mingorance, J., Tadros, M., Vicente, M., Gonzalez, J. M., Rivas, G., and Velez, M. (2005) Visualization of single *Escherichia coli* FtsZ filament dynamics with atomic force microscopy. *J. Biol. Chem. 280*, 20909–20914.
15. Margolin, W. (2005) FtsZ and the division of prokaryotic cells and organelles. *Nat. Rev. Mol. Cell Biol. 6*, 862–871.
16. Sanchez, M., Valencia, A., Ferrandiz, M. J., Sander, C., and Vicente, M. (1994) Correlation between the structure and biochemical activities of FtsA, an essential cell division protein of the actin family. *EMBO J. 13*, 4919–4925.
17. Erickson, H. P. (2001) The FtsZ protofilament and attachment of ZipA: Structural constraints on the FtsZ power stroke. *Curr. Opin. Cell Biol. 13*, 55–60.
18. Hale, C. A., and de Boer, P. A. (1997) Direct binding of FtsZ to ZipA, an essential component of the septal ring structure that mediates cell division in *E. coli*. *Cell 88*, 175–185.
19. Hale, C. A., Rhee, A. C., and de Boer, P. A. (2000) ZipA-induced bundling of FtsZ polymers mediated by an interaction between C-terminal domains. *J. Bacteriol. 182*, 5153–5166.
20. Ohashi, T., Hale, C. A., de Boer, P. A., and Erickson, H. P. (2002) Structural evidence that the P/Q domain of ZipA is an unstructured, flexible tether between the membrane and the C-terminal FtsZ-binding domain. *J. Bacteriol. 184*, 4313–4315.
21. Hale, C. A., and de Boer, P. A. (1999) Recruitment of ZipA to the septal ring of *Escherichia coli* is dependent on FtsZ and independent of FtsA. *J. Bacteriol. 181*, 167–176.
22. RayChaudhuri, D. (1999) ZipA is a MAP-Tau homolog and is essential for structural integrity of the cytokinetic FtsZ ring during bacterial cell division. *EMBO J. 18*, 2372–2383.
23. Hale, C. A., and de Boer, P. A. (2002) ZipA is required for recruitment of FtsK, FtsQ, FtsL, and FtsN to the septal ring in *Escherichia coli*. *J. Bacteriol. 184*, 2552–2556.
24. Haney, S. A., Glasfeld, E., Hale, C., Keeney, D., He, Z., and de Boer, P. (2001) Genetic analysis of the *Escherichia coli* FtsZ·ZipA interaction in the yeast two-hybrid system. Characterization of FtsZ residues essential for the interactions with ZipA and with FtsA. *J. Biol. Chem. 276*, 11980–11987.
25. Moreira, I. S., Fernandes, P. A., and Ramos, M. J. (2006) Detailed microscopic study of the full zipA:FtsZ interface. *Proteins 63*, 811–821.
26. Mosyak, L., Zhang, Y., Glasfeld, E., Haney, S., Stahl, M., Seehra, J., and Somers, W. S. (2000) The bacterial cell-division protein ZipA and its interaction with an FtsZ fragment revealed by X-ray crystallography. *EMBO J. 19*, 3179–3191.
27. Moy, F. J., Glasfeld, E., Mosyak, L., and Powers, R. (2000) Solution structure of ZipA, a crucial component of *Escherichia coli* cell division. *Biochemistry 39*, 9146–9156.
28. Attri, A. K., Fernandez, C., and Minton, A. P. (2010) pH-dependent self-association of zinc-free insulin characterized by concentration-gradient static light scattering. *Biophys. Chem. 148*, 28–33.
29. Attri, A. K., Fernandez, C., and Minton, A. P. (2010) Self-association of Zn-insulin at neutral pH: Investigation by concentration gradient−static and dynamic light scattering. *Biophys. Chem. 148*, 23–27.
30. Attri, A. K., and Minton, A. P. (2005) Composition gradient static light scattering: A new technique for rapid detection and quantitative characterization of reversible macromolecular hetero-associations in solution. *Anal. Biochem. 346*, 132–138.
31. Attri, A. K., and Minton, A. P. (2005) New methods for measuring macromolecular interactions in solution via static light scattering: Basic methodology and application to nonassociating and self-associating proteins. *Anal. Biochem. 337*, 103–110.
32. Kameyama, K., and Minton, A. P. (2006) Rapid quantitative characterization of protein interactions by composition gradient static light scattering. *Biophys. J. 90*, 2164–2169.
33. Cole, J. L., Lary, J. W., P Moody, T., and Laue, T. M. (2008) Analytical ultracentrifugation: Sedimentation velocity and sedimentation equilibrium. *Methods Cell Biol. 84*, 143–179.
34. Minton, A. P. (1997) Alternative strategies for the characterization of associations in multicomponent solutions via measurement of sedimentation equilibrium. *Prog. Colloid Polym. Sci. 107*, 11–19.